Exp Oncol 2021
43, 1, 15–20

Experimental ONCOLOGY

# MACROPHAGE POLARIZATION IN DYNAMICS OF LEWIS LUNG CARCINOMA GROWTH AND METASTASIS

*A.V. Chumak*, N.I. Fedosova, N.L. Cheremshenko, T.V. Symchych, I.M. Voyeykova, V.F. Chekhun*
*R.E. Kavetsky Institute of Experimental Pathology, Oncology and Radiobiology of NAS of Ukraine, Kyiv 03022, Ukraine*

***Aim:*** **To assess the functional state of macrophages based on various manifestations of their activity at the different stages of metastatic tumor growth in C57Bl mice.** ***Materials and Methods:*** **On days 7, 14, 21 and 28 after Lewis lung carcinoma transplantation to C57Bl mice, macrophages from various anatomic sites were isolated and tested on their cytotoxicity, metabolic activity, NO production and arginase activity.** ***Results:*** **In the populations of peritoneal and splenic macrophages, on days 7 and 21 of tumor growth antitumor (M1) cells prevailed while on days 14 and 28 tumor-promoting (M2) macrophages predominated. In the population of lung macrophages, cells with M1 phenotype were in the majority in the early stages of tumor growth. On days 21 and 28, M1 cells were gradually substituted by cells exhibiting M2 phenotype. This shift correlated with metastasis to lungs.** ***Conclusion:*** **Lewis lung carcinoma growth is accompanied by the gradual change in macrophage polarization from antitumor (M1) towards tumor-promoting (M2) type. These changes were more evident in population of lung macrophages and correlated with the parameters of metastasis.**
***Key Words:*** **Lewis lung carcinoma, C57Bl mice, macrophages, functional activity, metastasis.**

**DOI: 10.32471/exp-oncology.2312-8852.vol-43-no-1.15829**

Cancer progression is accompanied by the systemic effects in the host, with the immune system being involved [1, 2]. Tumor tissue is not homogeneous — it consists of different cell types: malignant (forming the main part of tumor or metastases) and normal cells of the body (tumor microenvironment), making tumor stroma. Tumor microenvironment also includes immune cells especially those constituting innate immune system — macrophages (Mph), neutrophils, natural killer cells. Mph representing the considerable part of immune cells in tumor microenvironment affect tumor-microenvironment relations during all the stages of tumor development. Nevertheless, their role in cancer is ambiguous [3].

Mph belong to the mononuclear phagocyte system. Nowadays, the term mononuclear phagocyte system refers to the family of cells of myeloid origin comprising bone marrow progenitors, blood monocytes, tissue Mph and dendritic cells [4–6]. Mph represent a big heterogeneous cells population. Depending on the tissue of residence and the surrounding microenvironment, Mph can exhibit different properties [7, 8]. Current Mph classification considers their anatomical niches of residence/functioning and activation signals, which allows dividing them into subtypes [9]. In general, these cells are divided into two populations: tissue residential and monocyte-derived infiltrating Mph [10, 11]. Tissue Mph are believed to be the progeny of the myeloid bone marrow cells, which give rise to circulating blood monocytes through consecutive stages of differentiation. The latter constantly migrate into peripheral tissues, where they differentiate into Mph [12]. However, by now it is shown that the majority of tissue-resident Mph population arises in embryonic development (originate from erythromyeloid precursors of the yolk sac) and self-maintains due to local proliferation rather than monocyte extravasation [13]. In particular, it was demonstrated that Mph resident in brain, lungs, liver, abdominal cavity and spleen are not differentiated from monocytes, but originate from embryonic precursors [11, 14]. On the other hand, classical monocytes (proinflammatory, $Ly6C^{high}$ monocytes) serve as a source for infiltrating Mph, which function in various pathological settings including cancer [15, 16].

Today, the origin of resident Mph subsets in different compartments of the body is still the subject of discussion. It does not seem to be always correct to classify these cells according to M1 and M2 (respectively, classically activated, proinflammatory and alternatively activated, anti-inflammatory) cell phenotypes [17]. While the mechanisms of M1 and M2 Mph activation and polarization are well described, the problem of functional state and polarization of resident Mph subsets in different anatomical niches during cancer progression remains to be elucidated. We have previously described the changes in the functional activity of Mph isolated from peritoneal cavity, spleen and tumor of mice bearing Ehrlich carcinoma [18]. The aim of this research was to assess the functional state of Mph based on various manifestations of their activity (cytotoxic and metabolic activity, nitric oxide (NO) production, arginase (Arg) activity) at different

Submitted: February 28, 2021.
*Correspondence: E-mail: immunomod@ukr.net
*Abbreviations used:* Arg – arginase; CTA – cytotoxic activity; CTAI – cytotoxic activity index; IL – interleukin; LLC – Lewis lung carcinoma; Mph – macrophages; NBT – nitroblue tetrazolium; NO – nitric oxide; OD – optical density.

stages of metastatic Lewis lung carcinoma (LLC) growth.

## MATERIALS AND METHODS

***Animals.*** The male C57Bl mice 2–2.5 month old weighting 19–20 g from the breeding facility of R.E. Kavetsky Institute of Experimental Pathology, Oncology and Radiobiology were used in the study. The experiments were performed in accordance with standard international rules on biologic ethics, the European Convention for the Protection of Vertebrate Animals Used for Experimental and Other Scientific Purposes [19] and the regulations approved by Institutional Animal Care and Use Committee.

***Experimental tumor.*** The strain of metastasizing LLC used in the experiment [20] was kindly granted by the R.E. Kavetsky Institute of Experimental Pathology, Oncology and Radiobiology Bank of Cell Lines from Human and Animal Tissues.

***Design of experiment.*** On day 0, C57Bl mice (n = 20) were injected with LLC cells in the hind foot ($4 \times 10^5$ cells/mouse) and followed till day 28 after tumor transplantation. The frequency (%) and latent period of tumor appearance, the tumor volume ($mm^3$), proportion of mice with metastases (%), number and volume of metastases ($mm^3$) were recorded [21]. Immunological testing was performed on days 7, 14, 21 and 28 after tumor challenge. Mph from different anatomical niches were obtained and functionally tested. Peritoneal, spleen and lung Mph were assessed for NO production and Arg activity. Peritoneal and spleen Mph were tested for the metabolic and cytotoxic activities too. Intact mice of the same strain, age and sex (n = 12) were used as the control group (referred to as the intact control).

***Isolation of Mph.*** Peritoneal and spleen Mph were isolated as described in [18]. In order to obtain lung Mph, aseptically removed lungs were homogenized with Potters homogenizer in medium 199 supplemented with 10% of bovine serum (Sigma, USA). Cell suspensions were centrifuged (550 g, 10 min) and resuspended in medium 199. After counting, $1 \times 10^6$ cells were placed on flat-bottomed plates and cultured for 2 h (37 °C, 5% $CO_2$, 100% humidity). Thereafter, non-adherent cells were removed, and the adherent cells were washed twice with 0.9% NaCl and taken for further investigation.

***Cytotoxic activity (CTA) assay.*** CTA was determined by MTT assay [22]. LLC cells were used as a target. In brief, target cells ($2 \times 10^4$ cell/well) in RPMI 1640 medium supplemented with 10% fetal bovine serum (all reagents from Sigma, USA) and antibiotics were placed in a flat-bottom 96-well plates where Mph ($4 \times 10^5$ cell/well) were adhered beforehand, and incubated for 18 h at 37 °C in a 100% humidity atmosphere with 5% $CO_2$. Control wells contained target cells or adhered Mph only. Then 0.01 ml of MTT solution/well (5 mg/ml, Sigma, USA) was added, and incubation continued for 2 h. Then the plates were centrifuged (550 g for 15 min) and washed twice with 0.9% NaCl solution. After that, 0.12 ml of 2 M KOH and 0.14 ml of dimethyl sulfoxide (50% solution) were added into each well. Optical density (OD) was measured at λ = 545 nm *vs* λ = 630 nm using a microplate ELISA reader (StatFax-2100, USA). Each sample was done in triplicate. CTA index (CTAI, %) was calculated by the formula:

$$CTAI = [1 - (OD_{mph+tc} - OD_{mph})/(OD_{tc} - OD_{blank})] \cdot 100\%,$$

where $OD_{mph}$ — optical density (OD) in wells containing only adhered Mph; $OD_{tc}$ — OD in wells containing only tumor cells; $OD_{mph+tc}$ — OD in wells wherein tumor cells and Mph where incubated; $OD_{blank}$ — OD in wells with the culture medium only.

***Metabolic activity examination.*** Mph metabolic activity was assessed by nitroblue tetrazolium (NBT) test as described previously with some modification [23]. In brief, Mph ($1 \times 10^6$ cell/ml, 0.2 ml/well) were incubated with 0.2% NBT solution (0.02 ml/well, Sigma, USA). After incubation (1 h, 5% $CO_2$, 37 °C), the plates were washed two times with 0.9% NaCl solution. The 2 M KOH solution (0.06 ml/well) and 50% DMSO solution (0.07 ml/well) were used to dissolve diformazan granules. OD was measured at λ = 630 nm with the use of a micro ELISA reader (StatFax-2100, USA). Each sample was done in triplicate. The results are presented as OD units (OU).

***NO production*** was measured by standard Griess reaction [24]. In brief, cell suspensions ($2 \times 10^6$ cell/well) were placed in a volume of 200 µl in 96-well flat-bottom tissue culture plates and cultured for 24 h. Each cell sample was investigated in duplicate. At the end of the incubation period, supernatants were collected and NO production was assessed by the accumulation of nitrite (as stable metabolite of NO) by Griess reaction. An aliquot of culture supernatant (100 µl) was mixed with an equal volume of Griess reagent (Acros Organics, Belgium) and incubated for 1 h at room temperature in the dark. The reaction products were colorimetrically quantified at λ = 550 nm. The standard curve plotted by the results of measurements of the solutions containing known concentration of $NaNO_2$ was used for converting the absorbance to micromolar concentrations of NO expressed in µM $NO_2$ per $10^6$ cells.

***Arg activity*** was determined based on urea measurement [24, 25]. Mph were lysed by double freezing and melting. Then 50 µl of 50 mM Tris-HCl (pH 7.4) and 10 µl of 50 mM $MnCl_2$ were added to each sample. Samples were incubated at 56 °C for 10 min, and upon addition of 100 µl of 0.5 M L-arginine (pH 9.7) further heated for 30 min (37 °C). The reaction was stopped with 800 µl of acidic mixture (1:3:7, 96% $H_2SO_4$ : 85% $H_3PO_4$ : $H_2O$). Then

40 μl of α-isonitrosopropriophenone (Sigma-Aldrich, USA) was added to the solution, which was heated for 30 min (95 °C) and incubated for 30 min at 4 °C. Urea concentration was measured spectrophotometrically at λ = 550 nm. Values of optical density were converted to mass of urea based on calibration curve of standard urea solution. Arg activity was calculated as described in [26]. One unit of Arg activity means the amount of the enzyme hydrolyzing 1 μM of arginine per 1 min. Results are expressed as units/$10^6$ cells.

***Statistical analysis.*** Statistical significance between groups was evaluated by nonparametric Mann — Whitney U test using Prism software Version 4.0. and assessed at $p < 0.05$. Correlation analysis between metastases volume, metastases number and NO production by lung Mph was determined by Pearson`s correlation coefficient using Prism software Version 4.0. Results are presented in box plots where whiskers mean maximum and minimum values, upper and lower borders of rectangles match the third and first quartiles respectively.

## RESULTS AND DISCUSSION

Throughout the experiment, the standard parameters of tumor growth (frequency, latent period of tumor appearance, tumor volume) and metastasis (proportion of mice with metastases, number and volume of metastases) were analyzed. The tumor yield reached 100% with the latency of 9.3 ± 1.2 days. The dynamics of tumor growth and metastasis in the lung within 28 days of observation were characteristic of this cancer model (Table).

In the intact mice, CTA of peritoneal or splenic Mph was almost the same with cytotoxicity index of 14.4% and 13.0%, respectively (Fig. 1). In the tumor-bearing mice, Mph isolated from different anatomical niches exhibited different functional activity depending on the day of tumor growth and the isolation source. CTA of the peritoneal Mph was elevated on day 7 of tumor growth ($p < 0.05$) and sharply decreased a week later (1.4 times lower as compared to the intact control). CTA of the splenic Mph on day 7 and 14 of tumor growth was 1.2 and 2.9 times lower ($p < 0.05$) as compared to the intact control level. On day 21, the CTA of peritoneal Mph was elevated as compared to the intact control, splenic Mph — increased to the level of intact control. On day 28, independently of the isolation source, CTA of Mph was below the intact control level (see Fig. 1, *a* and *b*).

The metabolic activity of Mph, examined by the NBT-reduction test, is depicted in Fig. 2. The metabolic activity of Mph changed in the same way whichever was the source of their isolation. As compared to the intact control, metabolic activity

**Table.** Tumor volume and metastasis parameters in LLC-bearing C57Bl mice

| Parameter | Day of tumor growth | | | |
|---|---|---|---|---|
| | 7 | 14 | 21 | 28 |
| Tumor volume, $mm^3$ | – | 77.0 ± 8.5 | 826.0 ± 270.1 | 1861.0 ± 238.8 |
| Metastases number, n | – | – | 4.3 ± 0.9 | 10.3 ± 0.3 |
| Metastases volume, $mm^3$ | – | – | 14.3 ± 0.9 | 41.2 ± 4.7 |

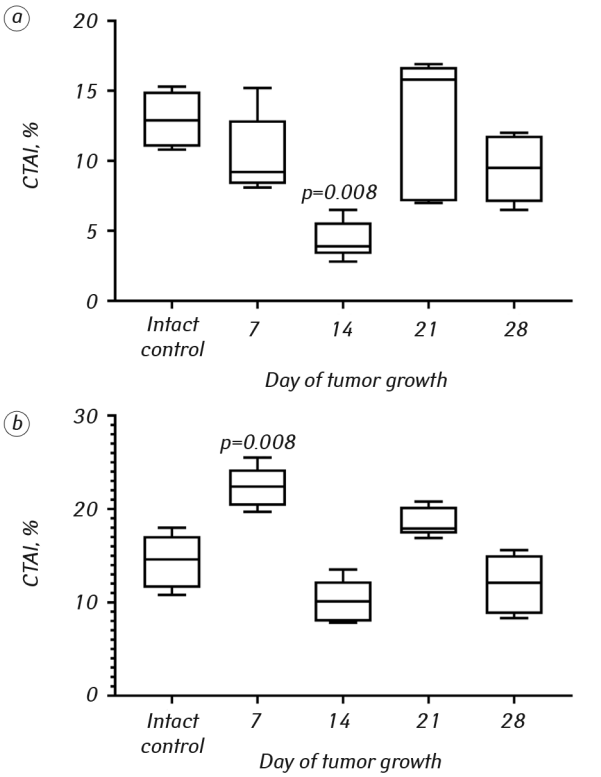


**Fig 1.** Changes in the cytotoxic activity of splenic (*a*) and peritoneal (*b*) Mph in LLC-bearing C57Bl mice. *P*-value were calculated as compared to intact control

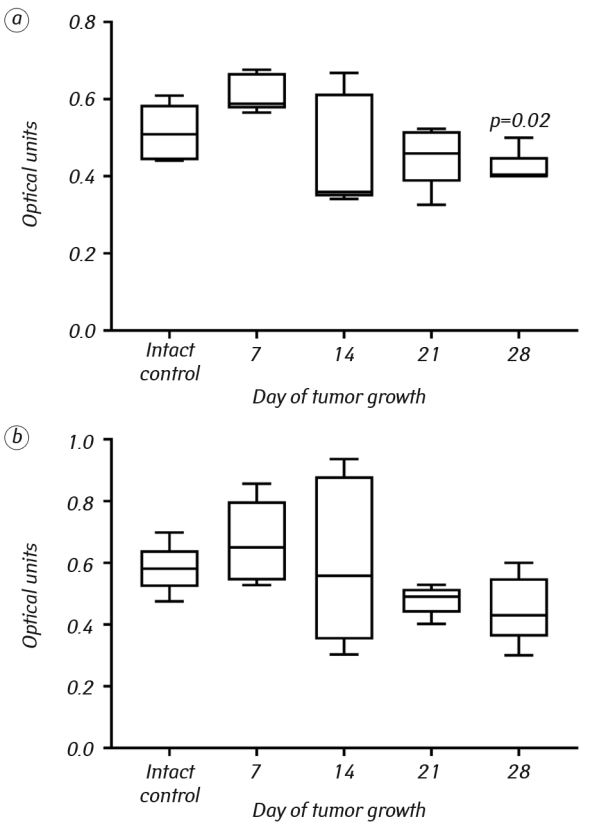


**Fig 2.** Changes in the metabolic activity in NBT-test of splenic (*a*) and peritoneal (*b*) Mph in LLC-bearing C57Bl mice. *P*-value were calculated as compared to intact control

of peritoneal and splenic Mph was elevated on day 7 of tumor growth and gradually declined at the end of the experiment.

As it is known, Mph play ambiguous role in cancer progression. During all the stages of cancer processes, they regulate the interplay between cancer cells and tumor microenvironment and are able to acquire different properties depending on the signals of the functioning environment. Depending on tissue microenvironment, Mph can polarize towards M1 or M2 phenotype, possessing pro-inflammatory or anti-inflammatory activities, respectively. We assessed the functional state of Mph based on their Arg- or NO-producing activities that allows us to distinguish between Mph polarization type.

In the intact C57Bl mice, Mph produced high levels of NO but low amounts of Arg independently of the isolation niche. NO/Arg ratio was 25.6, 26.8 and 27.8 for, respectively, peritoneal, spleen and lung Mph (Fig. 3). In the tumor-bearing mice, peritoneal and spleen Mph exhibited similar changes in their NO- and Arg-producing activities. On day 14 and 28 of tumor growth, production of NO by peritoneal Mph dropped by 31.7% and 28.6% comparing with the intact control. Splenic Mph production of NO was reduced by 27.1% on day 14 comparing with the intact control. It worth mentioning that on day 21 of tumor growth the production of NO by splenic Mph increased ($p < 0.05$) 1.1 times as compared to the intact control group. The highest Arg activity, on the contrary to NO production, was registered on days 14 and 28 of tumor growth. Lung Mph exhibited different dynamics of changes in NO and Arg production. On the early stages of tumor growth (days 7 and 14), NO/Arg ratio was 28.3 and 33.6 respectively. At further time points (day 21 and 28 of tumor growth) NO/Arg ratio was significantly declining ($p < 0.05$) due to the increase in Arg activity and statistically significant decrease in NO production.

Thus, analysis of the changes in the indices characterizing functional activity of Mph isolated from various anatomical niches (peritoneal cavity, spleen and lung) on different stages of LCC growth pointed to the gradual change in Mph polarization. In peritoneal and splenic Mph, antitumor (M1) Mph prevailed on days 7 and 21 of tumor growth while on days 14 and 28 tumor-promoting (M2) Mph came out on top. In the population of lung Mph, obtained data indicated the presence of M1 cells on the early stages of tumor growth (up to day 14); later (till day 28) their gradual polarization to the M2 phenotype was registered. Changes in functional polarization of lung Mph (from antitumor towards tumor-promoting) correlated with the metastasis initiation that is proved by Pearson correlation coefficient. Metastases volume and number inversely correlated with NO production by lung Mph (r = –0.92 and –0.89 respectively).

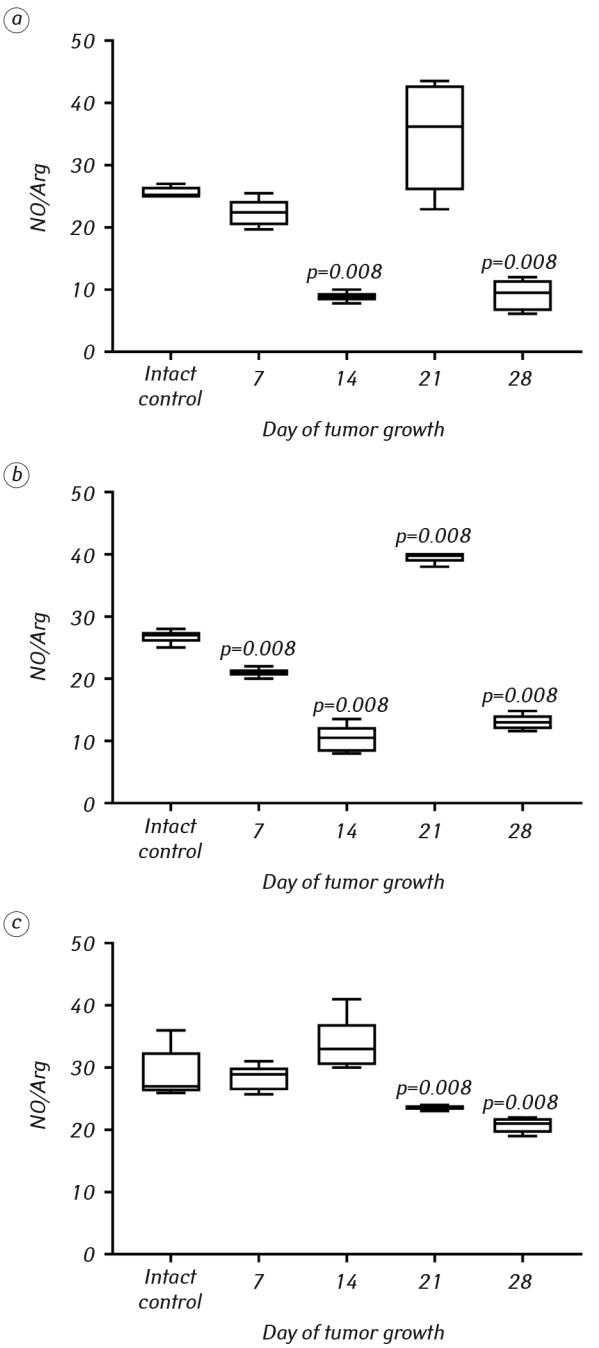


**Fig. 3.** Changes in NO/Arg ratio for various residential peritoneal (*a*), splenic (*b*) and pulmonary (*c*) Mph isolated from LLC-bearing C57Bl mice. *P*-value were calculated as compared to intact control

Correlation between metastasis parameters and the activity of peritoneal and splenic Mph was insignificant.

It is known that the tumor process is accompanied by the development of local and systemic inflammation with the expression of proinflammatory transcription factors in tumor cells (such as NF-κB, STAT3, HIF-1α), which determine the production of spectrum of cytokines, chemokines and inflammatory enzymes in the tumor microenvironment, as well as the influence of these factors on the immune response.

As the effectors of the innate immune response, Mph are able to response on wide spectrum of stimuli: viral, bacterial, parasitic antigens, immune complexes, antigens of apoptotic or necrotic cells, soluble mediators produced by other cells. The direction of resident Mph polarization depends on the signals of the local microenvironment, such as components of damaged cells, cytokines and chemokines of activated lymphocytes, microbial products. In particular, affected by lipopolysaccharide, interferon-gamma and granulocyte-macrophage colony-stimulating factor Mph are polarized to M1 phenotype and acquire the ability to secrete significant amounts of proinflammatory cytokines (interleukin (IL)-1-beta, tumor necrosis factor, IL-12, IL-18 and IL-23), which promotes the involvement in the immune response of lymphocytes taking part in antigen-specific inflammatory reactions (Th1 and Th17) [2, 27, 28]. Such gradual, associated with changes in production of humoral factors, mutual activation of lymphocytes and Mph possibly explains the increase in number of M1-polarized cells on day 21 of tumor growth registered in this experiment. Later, due to the increase in production of tumor-promoting cytokines (IL-6, IL-17, IL-23, epidermal growth factor receptor, transforming growth factor-β), Mph polarization towards M2 phenotype emerged on day 28 of tumor growth.

Gradual polarization from M1 toward M2 phenotype was more evident for lung Mph and correlated strongly with the metastasis parameters. This finding can underline new approaches to reducing the metastasis by influencing the direction of Mph polarization.

## REFERENCES


1. **Mc Allister S**, **Weinberg R.** The tumour-induced systemic environment as a critical regulator of cancer progression and metastasis. Nat Cell Biol 2014; **16**: 717–27.

2. **Paul D.** The systemic hallmarks of cancer. J Cancer Metastasis Treat 2020; **6**: 29; http://dx.doi.org/10.20517/2394-4722.2020.63.

3. **Weagel E, Curren S, Liu PG, *et al.*** Macrophage polarization and its role in cancer. J Clin Cell Immunol 2015; **6**; http://dx.doi.org/10.4172/2155-9899.1000338.

4. **Titov LP.** Monocytes, macrophages, dendritic and myeloid suppressor cells: genesis, classification, immunobiological properties. Proc Natl Acad Sci Belarus. Medical series 2018; **15**: 363–82.

5. **Geissmann F, Gordon S, Hume DA, *et al.*** Unravelling mononuclear phagocyte heterogeneity. Nat Rev Immunol 2010; **10**: 453–60.

6. **Cassado A, D'Império Lima MR, Bortoluci KR**. Revisiting mouse peritoneal macrophages: heterogeneity, development, and function. Front Immunol 2015; **6**: 225; 10.3389/fimmu.2015.00225.

7. **Movahedi K, Laoui D, Gysemans C, *et al.*** Different tumor microenvironments contain functionally distinct subsets of macrophages derived from Ly6C (high) monocytes. Cancer Res 2010; **70**: 5728–39.

8. **Richards DM, Hettinger J, Feuerer M.** Monocytes and macrophages in cancer: development and functions. Cancer Microenviron 2013, **6**: 179–91.

9. **Murray PJ, Allen JE, Biswas SK, *et al.*** Macrophage activation and polarization: nomenclature and experimental guidelines. Immunity 2014; **41**: 14–20.

10. **Chen B, Brickshawana A, Frangogiannis NG.** The functional heterogeneity of resident cardiac macrophages in myocardial injury CCR2(+) cells promote inflammation, whereas CCR2(-) cells protect. Circ Res 2019; **124**: 183–5.

11. **Honold L, Nahrendorf M.** Resident and monocyte-derived macrophages in cardiovascular disease. Circ Res 2018; **122**: 113–27.

12. **Das A, Sinha M, Datta S, *et al.*** Monocyte and macrophage plasticity in tissue repair and regeneration. American J Pathol 2015; **185**: 2596–605.

13. **Lavin Y, Mortha A, Rahman A, Merad M.** Regulation of macrophage development and function in peripheral tissues. Nat Rev Immunol 2015; **15**: 731–44.

14. **Ginhoux F, Guilliams M.** Tissue-resident macrophage ontogeny and homeostasis. Immunity 2016; **44**: 439–49.

15. **Liao X, Shen Y, Zhang R, *et al.*** Distinct roles of resident and nonresident macrophages in nonischemic cardiomyopathy. Proc Natl Acad Sci U S A 2018; **115**: E4661–9.

16. **Hashimoto D, Chow A, Noizat C, *et al.*** Tissue-resident macrophages self-maintain locally throughout adult life with minimal contribution from circulating monocytes. Immunity 2013; **38**: 792–804.

17. **Ghosn EE, Cassado AA, Govoni GR, *et al.*** Two physically, functionally, and developmentally distinct peritoneal macrophage subsets. Proc Natl Acad Sci USA 2010; **107**: 2568–73.

18. **Symchych TV, Fedosova NI, Chumak AV, *et al.*** Functions of tumor-associated macrophages and macrophages residing in remote anatomical niches in Ehrlich carcinoma bearing mice. Exp Oncol 2020; **42**: 197–203.

19. **Kozhemyakin YM, Khromov OS, Filonenko MA, Sayfutdinova HA.** Guideline on management of laboratory animals and work with them. Kyiv: Avitsena, 2002. 179 p. (in Ukrainian).

20. **Treschalina EM.** Antitumor activity of substances of natural origin. Practical Medicine, 2005. 270 p. (in Russian).

21. **Turusov VS.** Methods for the detection and regulation of chemical carcinogens. Moscow: Medicine, 1986. 152 p. (in Russian).

22. **Mosmann T.** Rapid colorimetric assay for cellular growth and survival: application to proliferation and cytotoxicity assays. J Immunol Methods 1983; **65**: 55–63.

23. **Van de Loosdrecht AA, Beelen RH, Ossenkoppele GJ, *et al.*** A tetrazolium-based colorimetric MTT assay to quantitate human monocyte mediated cytotoxicity against leukemic cells from cell lines and patients with acute myeloid leukemia. J Immunol Methods 1994, **174**: 311–20.

24. **Reiner NE.** Macrophages and Dendritic Cells. Methods and Protocols. Humana Press, 2009. 368 p.

25. **Corraliza IM, Campo ML, Soler G, Modolell M.** Determination of arginase activity in macrophages: amicromethod. J Immunol Methods 1994; **174**: 231–5.

26. **Dovgiy RS, Shitikov DV, Pishel IN, *et al.*** Functional state and metabolic polarization of splenic macrophages of old immunized mice. Problemy Stareniya Dolgoletiya 2015; **24**: 147 (in Ukrainian).

27. **Rőszer T.** Understanding the mysterious M2 macrophage through activation markers and effector mechanisms. Mediators of Inflammation 2015; **2015**: ID 816460. https://doi.org/10.1155/2015/816460

28. **Davis MJ, Tsang TM, Qiu Y, *et al*.** Macrophage M1/M2 polarization dynamically adapts to changes in cytokine microenvironments in Cryptococcus neoformans infection. mBio 2013; **4**: e00264–13.

## ЗМІНИ ПОЛЯРИЗАЦІЇ МАКРОФАГІВ У ДИНАМІЦІ РОСТУ МЕТАСТАЗУЮЧОЇ КАРЦИНОМИ ЛЬЮЇС

***А.В. Чумак*, Н.І. Федосова, Н.Л. Черемшенко, Т.В. Симчич, І.М. Воєйкова, В.Ф. Чехун***

*Інститут експериментальної патології, онкології та радіобіології ім. Р.Є. Кавецького НАН України, Київ 03022, Україна*

***Мета*:** Оцінити стан макрофагів мишей лінії C57Bl за різними проявами їх функціональної активності на різних стадіях росту метастазуючої пухлини. ***Матеріали та методи*:** У дослідженні використовували мишей лінії C57Bl з епідермоїдною метастазуючою карциномою легені Льюїс. На 7-, 14-, 21- та 28-й день після перещеплення пухлини макрофаги з різних ніш були виділені та піддані функціональному аналізу. ***Результати*:** Макрофаги, отримані з різних біологічних ніш у інтактних тварин, за дослідженими показниками функціональної активності мали фенотип M1. У популяціях макрофагів, отриманих з селезінки та перитонеальної порожнини мишей лінії C57Bl на 7-і 21-шу доби росту карциноми легені Льюїс переважали клітини з протипухлинними властивостями (M1), на 14- та 28-му добу — клітини з пропухлинними властивостями (M2). У популяції легеневих макрофагів на ранніх стадіях пухлинного процесу переважали клітини з фенотипом M1, до 28-ї доби спостерігали поступову їх поляризацію до фенотипу M2. Такі зміни корелювали з показниками метастазування в легені в ці терміни. ***Висновок*:** Аналіз показників функціональної активності макрофагів свідчить про їх поступову поляризацію від клітин з проти- (M1) до клітин з пропухлинними (M2) властивостями в динаміці росту карциноми легені Льюїс. Виявлені зміни були найбільш вираженими в популяції легеневих макрофагів та мали кореляційний зв`язок з показниками метастазування.

***Ключові слова*:** карцинома легені Льюїс, миші лінії C57Bl, макрофаги, функціональна активність, метастазування.